Understanding very faint X-ray binaries from X-ray light curves

Simon van Eeden

Supervised by Nathalie Degenaar

ABSTRACT

X-ray binaries known as accreting neutron stars and black holes include a selection of sources that appear as very faint having peak luminosity's of 10^{34-36} erg s^{-1}. Very faint X-ray binaries reach the limits of X-ray instrumental sensitivity which hampered detailed studies and therefore remain poorly understood. Possible explanations for their very faint character are that they have short orbital periods or a different accretion process from bright sources. To find out more about the nature of these objects we have performed a first systematic analysis on accretion outburst light curves from 21 sources by determining the duration and decay time. We found that the distribution of the duration and decay time of each outburst appears very similar to bright X-ray binaries hinting to a similar accretion process. We have furthermore used the disc instability model to probe the accretion disc radius and orbital period and found short orbital periods of two to six hours for 6 sources. We have shown that the disc instability model can be used on outburst light curves that have sufficient number of observations. Therefore to further investigate the potential of this model we recommend to obtain sensitive X-ray observations of 1 to 3 days on new outbursts from very faint x-ray binaries.

images/logo-combi-vu-uva-nl.png

Populaire samenvatting

Röntgendubbelster systemen bestaan uit een neutronen ster of een zwart gat en een donor ster die om elkaar heen draaien. Doordat neutronon sterren en zwarte gaten zo compact zijn kan hun extreme zwaartekracht materie van de buitenste lagen van de donor ster naar hen toe trekken. Hierdoor ontstaat er een stroom van materie richting het compacte object wat we ook wel accretie noemen. Deze stroom orienteerd zich dusdanig dat er een schijf met materie ontstaat rondom het compacte object. Door instabiliteit in deze schijf kunnen er uitbarstingen ontstaan waarbij in een aantal dagen tot weken erg veel materie op het compacte object valt. Tijdens een uitbarsting wordt er meer röntgenstraling uitgezonden wat we met röntgen telescopen in de ruimte zoals Swift en RXTE kunnen waarnemen.

In dit onderzoek is gekeken naar 21 röntgendubbelster systemen die erg zwak zijn. We weten nog tot nu nog niet waarom deze systemen zo zwak zijn. Mogelijke verklaringen hiervoor zijn dat vergeleken met heldere bronnen de omlooptijd veel kleiner is of dat de accretiestroom heel anders is. Om dit beter te begrijpen hebben we van deze systemen het helderheidsverloop van uitbarstingen gekarakteriseert, iets wat tot nu toe alleen nog voor heldere bronnen gedaan is. Als eerst hebben we gekeken of uitbarstingen van deze bronnen een andere lengte en afvaltijd hebben in vergelijking met heldere bronnen. We hebben gevonden dat de distributie van de lengte en de afvaltijd in hele zwakke systemen dezelfde trend volgt als die van heldere systemen. We denken dat dit een indicatie geeft dat hele zwakke systemen hetzelfde accretie process volgen als heldere systemen.

Ten tweede hebben we gebruik gemaakt van een stabiliteits model om de omlooptijd van het systeem te kunnen bepalen omdat we verwachten dat deze korter is voor zwakkere systemen. Echter geldt voor veel hele zwakke bronnen dat het helderheidsverloop van een uitbarsting niet altijd duidelijk te bepalen is omdat ze zo zwak zijn en het interval tussen observaties een aantal dagen tot een week is. Het model lijkt voor zes systemen die een duidelijk helderheidsverloop laten zien de uitbarsting vorm goed te benaderen. Alle zes systemen hebben een kortere omlooptijd van 2 tot 6 uur wat overeenkomt met een van de verwachtingen. Dit geeft ons ook een indicatie voor een vergelijkbaar accretieprocess in hele zwakke en heldere systemen. Voor 2 bronnen geeft het model resultaten die overeenkomen met onafhankelijke observaties. Dit suggereert dat het model gebruikt kan worden om meer te weten te komen over de accretie eigenschappen van hele zwakke systemen. Om dit verder te onderzoeken zijn er meer observaties in X-ray nodig waarbij gekeken wordt met een observatie interval van 1 tot 3 dagen zodat het helderheidsverloop duidelijk te zien is.

1 Introduction

The majority of all stars are part of a binary system in which two stars orbit the center of mass. A special case of binary systems are X-ray binaries which contain a neuron star (NS) or a black hole (BH) and a donor star. The strong gravitational forces from these compact objects can cause accretion of matter from the donor star on to the compact object (shown in figure 1).
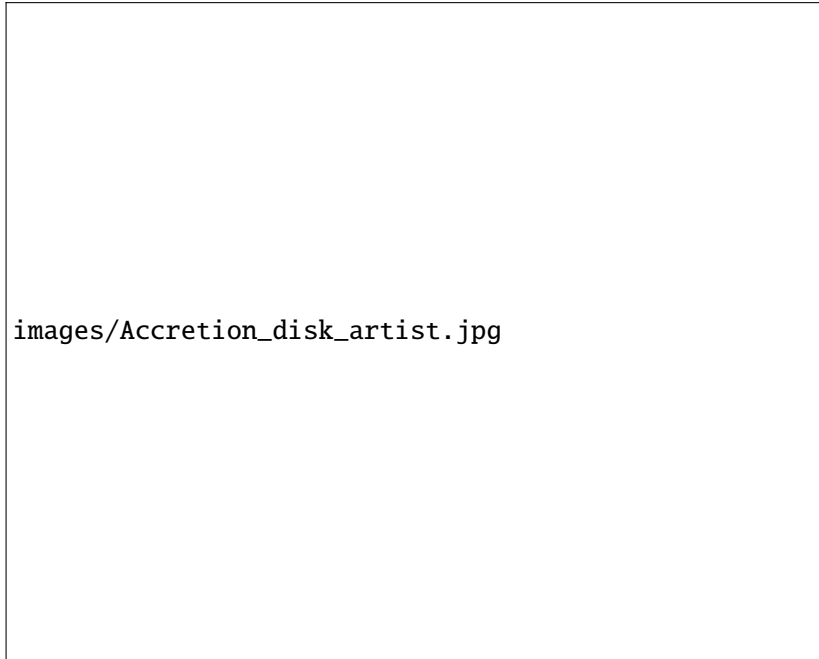

Fig. 1: Artist impression of an accreting X-ray binary.

During accretion gravitational potential energy is converted into radiation mostly in X-rays which can be observed with X-ray telescopes. Observations have shown persistent sources that have a continuous accretion rate and emit continuous X-rays. However they also show transient sources that are most of the time in quiescence with little accretion and occasionally show a rise in X-ray. These occasional events are called outbursts and typically last for a couple of days to several months while reaching peak luminosity's up to 10^{39} erg s^{-1}. Outbursts are caused by thermal-viscous instabilities in the accretion disk described by the disc instability model (Lasota 2001; Hameury 2020). Currently roughly 200 X-ray binaries have been observed (see Liu et al. 2007 for an overview up to 2007, with a few systems discovered since then). Since the last 15 years evidence have grown for the existence of Very Faint X-ray Binaries (VFXBs) that have outburst peak luminosities of 10^{34-36} erg s^{-1} 2-10 keV (Wijnands et al. 2006). For a long time, detailed studies on this subclass were difficult because their faintness approaches the instrumental sensitivity limits. Despite the observational difficulties currently about 30 X-ray binaries are classified as a VFXB.

It is yet not understood why VFXBs are so faint. Two possible explanations for there faintness are that they have short orbital periods (King and Wijnands 2006; in 't Zand, J. J. M. et al. 2007; Wu et al. 2010; Hameury and Lasota 2016) or a different accretion process (Heinke et al. 2009; Degenaar et al. 2014; Heinke et al. 2015) compared to bright X-ray binaries. So far research have been focusing only on individual sources but to find out more about the origin of the faint character it is worthwhile

to perform a systematic analysis on outburst light curves from multiple VFXBs. There have been already systematic studies of outbursts from bright X-ray binaries (24 sources in Chen et al. 1997; 36 sources in Yan and Yu 2015) in which they determined distributions for the e-folding rise and decay timescale, duration and total radiated energy of each outburst. Comparing outburst characteristics such as the duration and decay time of VFXBs with those of bright sources can provide us more insight in potential differences in the accretion process of these two sub classes.

So far the disc instability model has described the decay shape of several outbursts from bright sources (Powell et al. 2007 on ten sources, one of them shown in figure 2) and for a handful of VFXBs (Heinke et al. 2015 on two sources) it has proved to be a tool to test if VFXBs have short orbital periods. It is therefore interesting to test the disc instability model on more VFXBs and find out if they have short orbital periods.
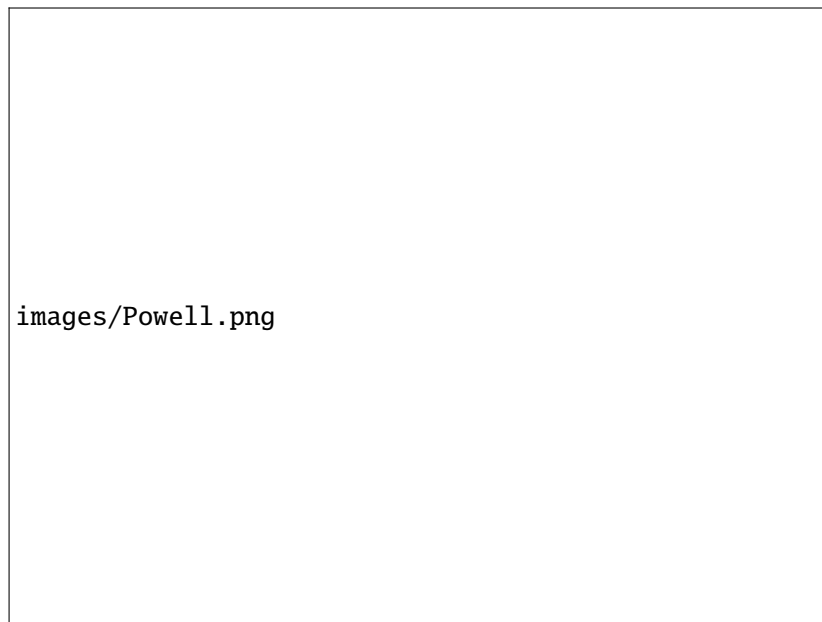

images/Powell.png

Fig. 2: The light curve of GRO J 1655-40 fitted to the disc instability model, from Powell et al. 2007.

To fulfill these needs in exploring the nature of very faint x-ray binaries, we aim to answer the following two questions. What is the typical duration and decay time of outbursts of VFXBs? Do VFXBs have shorter orbital periods?

2   X-ray binary classification

This section contains the required background knowledge in the classification of X-ray binaries. The classification of X-ray binaries involves three criteria: the type of the compact object, the mass of the companion star and the X-ray peak luminosity. The following sections will explain each criteria.

2.1   Type of the compact object

Black hole
The first classification criteria is the type of compact object; BH or NS. BH's can be identified by

the mass of the compact object. If in NSs the mass becomes higher then $\sim 2.5 - 3M_\odot$ depending on the equation of state (Baiotti et al. 2008), the neutron degeneracy pressure can not balance the gravitational force anymore. Therefore if the mass of the compact object exceeds $\sim 2.5 - 3M_\odot$ the compact object must be a BH. Calculating the mass of the compact object can be a hard task because in order to identify the spectra of the donor star the X-ray binary must be bright enough in quiescence. It his is the case the orbital period can be extracted from a radial velocity curve from the donor star. The radial velocity curve originate from the fact that if the orbital plane is aligned with our line of sight the spectral lines are blue shifted when the donor star moves towards us and red shifted when the donor star moves away from us. Knowing the period and assuming a that the inclination is 90 degrees and the mass of the donor star is zero the mass function from the laws of Kepler gives the minimum mass of the compact object. If this mass exceeds $3M_\odot$ the compact object must be a BH. This method resulted in the identification of several tens of BH X-ray binaries (Corral-Santana et al. 2016; Tetarenko et al. 2016) with XTE J1118+480 as VFXB (Torres et al. 2004).

Neutron star

In contrast to a BH that has a event horizon, a NS has a solid surface and a magnetic field which give rise to thermonuclear X-ray bursts (Cornelisse et al. 2002) and X-ray pulsations (Ng et al. 2021). During a thermonuclear burst material piles up at the surface and eventually detonates resulting in a bright and short flash in X-ray (shown in figure 3).
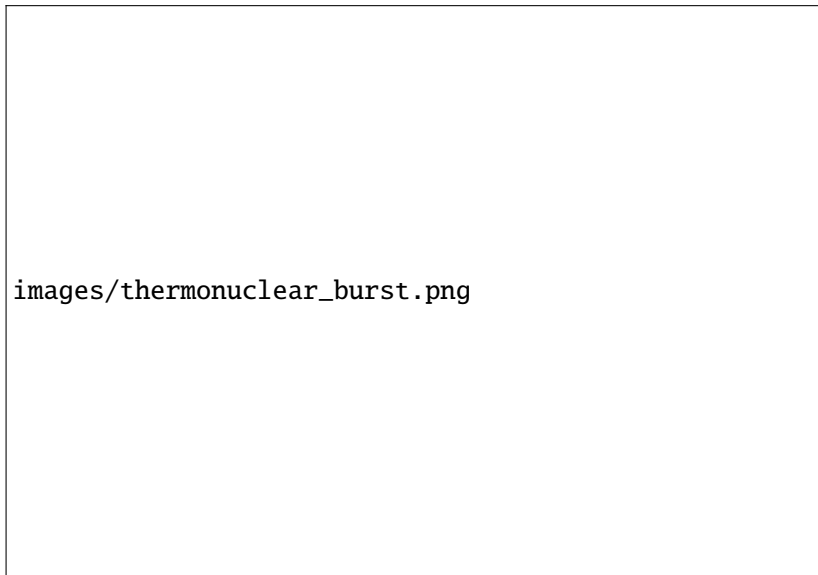

Fig. 3: Example of a typical thermonuclear burst observed in 4U 1735 - 445 (Tournear et al. 2008).

X-ray pulsations originate from the magnetic field in combination with the spin of a NS. The magnetic field forces material from the accretion disc to move along the magnetic field lines and end up at the magnetic poles. While material falls onto the poles they heat up and shine brighter which causes X-ray pulsations when the NS spins in our line of sight.

2.2   Mass of companion star

Low mass or high mass X-ray binaries

High mass X-ray binaries (HMXBs) can accrete material by a stellar wind or decretion disk of the

companion star. Be/X-ray binaries are the most common type for accretion via a decretion disk. These systems harbor a B or O type star that can spin so fast that the rotational force overcomes the gravitational force and a decretion disk forms (Okazaki and Negueruela 2001). HMXBs can also host a supergiant star that loses mass by a strong stellar wind. The material that is lost can be captured and accreted onto the compact object. In low mass X-ray binaries (LMXBs) mass transfer happens typically via Roche Lobe overflow during which a accretion disk forms around the compact object (see section 3 for more detail).

2.3   Luminosity

Bright
The third classification of X-ray transients is based on their X-ray peak luminosity when they are in outburst. Bright to very bright X-ray binaries have peak luminosity's of 10^{36-39} erg s^{-1} 2-10 keV. Currently the best description of the accretion behaviour of this class is given by the disc instability model explained in section 3. A large fraction of this subclass contain NS's. Also they are more concentrated towards the galactic center (Cornelisse et al. 2002). But this might be a consequence of observations mainly focusing on this region (Degenaar and Wijnands 2009).

Very Faint
Very Faint X-ray binaries have peak X-ray luminosity's of 10^{34-36} erg s^{-1}. There have been several suggestions for explaining the very faint character. They could be intrinsically bright but appear as very faint due to their large distance (Wijnands et al. 2006). Or if these systems are edge-on oriented the accretion disk can partly block X-rays (Muno et al. 2005). This way it appears as a very faint source but has a intrinsic luminosity that belongs to a bright source. Although it is more likely that these sources have a very faint intrinsic luminosity (Wijnands et al. 2006). As Wijnands et al. 2006 mentioned, different characteristics have been found in the analysis of light curves and spectra from VFXBs and it seems to be a inhomogeneous class including LMXBs and HMXBs, and with the distinction between bright and very faint rather arbitrary. However we currently know that that most sources in this class are LMXBs and those are studied here.

3   The disc instability model

For LMXBs accretion happens via Roche lobe overflow. While material from the outer layers of the companion star is transferred towards the compact object angular momentum must be conserved and a accretion disk forms (Frank et al. 2002). Instabilities in this accretion disc can trigger the rise of outbursts. The disc instability model is the accepted description of outbursts in LMXBs (King and Ritter 1998). This model includes the effects of the disc irradiation on the disc stability. Irradiation is caused by intense X-rays from the inner disk and for NSs the stellar surface may contribute as well.

The disc instability model provides predictions for the outburst decay shape depending on the ionization state of the accretion disk. At the start of every outburst the accumulation of matter in the accretion disc is able to ionize the disc. The ionization raises the disc's viscosity which causes rapid rise in X-ray flux. When the accretion disk is fully ionized by irradiation from the central source a exponential decay is predicted. As soon as the outer edge of the disc cools down below the hydrogen ionization temperature the accretion disk becomes partly ionized. During this stage a linear decay is expected until it fades to quiescence. The transition from exponential to linear decay happens at a

luminosity

$$L_t(NS) = 3.7 \times 10^{36} R_{11}^2 \text{erg s}^{-1} \tag{1}$$

for NS's and

$$L_t(BH) = 1.7 \times 10^{37} R_{11}^2 \text{erg s}^{-1} \tag{2}$$

for BHs (Shahbaz et al. 1998). With R_{11} the accretion disc radius in units of 10^{11} cm and L_t the transition luminosity. The difference is due to whether the stellar surface or the inner disk is the dominating source of irradiation. Section 4.3 provides a explanation of how physical parameters were extracted from this model.

4 Method

From the about 30 known VFXBs we selected light curves that show a outburst and have enough data points to reveal a outburst shape. The selected X-ray light curves cover data from two telescopes that are sensitive enough to detect outbursts in VFXBs and allow for daily observation intervals: the Rossi X-ray Timing Explorer (*RXTE*) which observed from 1996 until 2012 and the Neil Gehrels Swift Observatory (*Swift*) which is observing since 2005. All the light curves from *RXTE* contain continuous observations taken with the All Sky Monitor (*ASM*) [1] or with the the Proportional Counter Array (*PCA*) [2] (Swank and Markwardt 2001). The *PCA* and *ASM* have a energy range of 2–10 keV.

Six *Swift* light curves are from the galactic center observing campaign (Degenaar et al. 2015). The other *Swift* light curves are processed via the online tool from Evans et al. 2007. All *Swift* light curves contain series of observations typically triggered by reports of source activity. The X-ray telescope on board of *Swift* has two observing modes. Most of the time our sources are weak enough to be observed with the Photon Counting (*PC*) mode. But when the count rate reach a critical value of $\sim$1 c s^{-1} pile-up becomes an issue and *Swift* switches to Window Timing (*WT*) mode. In both modes the X-ray telescope on board *Swift* is sensitive to a energy range of 0.3-10 keV. For the analysis on the *Swift* light curves we have used data from both observing modes.

4.1 Outburst duration τ_{dur}

Based on the symmetry of most outburst shapes, each outburst is fitted to a Gaussian using the `astropy` package (Astropy Collaboration and Robitaille 2013) to determine the outburst duration. From each Gaussian fit the standard deviation (σ) is used to derive the duration of the outburst

$$\tau_{dur} = 6\sigma \tag{3}$$

with τ_{dur} the outburst duration and σ the standard deviation from the Gaussian fit. On most outbursts a Gaussian does not fit perfectly but it does provide a systematic way to roughly estimate the duration. In order to get the best fit possible we have extracted the average count rate and the standard deviation from fluctuations around the zero point:

1. **Fit-data selection**
   The standard deviation of fluctuations around the zero point is used as a threshold for noise detection in the following way. For each outburst, data points were selected from the peak to

---

[1] http://xte.mit.edu/asmlc/ASM.html
[2] https://asd.gsfc.nasa.gov/Craig.Markwardt//galscan/main.html

earlier and later times until two adjacent observations have count rates below 2σ. This selected region is used as the input data for the Gaussian fit. For some *Swift* light curves containing solely the outburst region we used all data points.

2. **Offset count rates**.
   In order to get the best possible fit the light curve should converge to a average count rate of zero similar to the Gaussian fit. Therefore all light curves count rates are subtracted by the average count rate of the fluctuations around the zero point. Light curves that only show the outburst region weren't corrected for zero point fluctuations.

For outbursts containing a few data points ($\sim$4) `astropy` can have trouble in finding the best fit and converge to amplitudes bigger then ten times the peak count rate. To avoid this behaviour the amplitude is constrained to

$$\text{amplitude} < 1.3 \times \text{peak rate} \tag{4}$$

4.2 Outburst decay time τ_{dec}

The second outburst parameter that is determined is the decay time τ_{dec}, also referred to the *e*-folding timescale computed over the outburst decay region (Chen et al. 1997). The decay time is, such as τ_{dur}, unrelated to instrumental sensitivity which makes it suitably for comparison between different sources from different telescopes. In order to extract τ_{dec} from each outburst, a exponential function was fitted, using the `astropy` package. The exponential fit function is defined as

$$F(t) = A \exp\left(-\frac{t}{\tau_{dec}}\right) \tag{5}$$

with $F(t)$ the count rate, A the amplitude, t the time after the start of the outburst decay and τ_{dec} is the decay time. As mentioned earlier, we fitted this decay model to the outburst decay region. This region is determined similarly as for τ_{dur} but the start point is fixed at the time of the peak count rate. For some *Swift* light curves that are containing solely the decay region the whole data set was used.

The fit function 5 converges to zero moving forward in time. So to obtain the best fit the light curves should have a average count rate of zero when in quiescence. This correction is performed by subtracting the average of the zero point fluctuations similar to τ_{dur}.

4.3 Decay model

We have used the accretion disc model described in Heinke et al. 2015 to fit outburst decay light curves. Therefore we applied python code[3] that contains all of the following. At the beginning of the outburst decay when the disc is completely ionized the light curve shows a exponential decay shape. At some time t_t the irradiation cannot maintain a fully ionized disc and the decay shape switches to linear. The exponential shape is described by

$$F(t) = (Ft - Fe) \exp\left(-\frac{t - t_t}{\tau_e}\right) + F_e \tag{6}$$

With $F(t)$ the count rate, F_t the count rate at the transition, F_e the exponential amplitude, t the time, τ_e the exponential decay time and t_t the time at the transition. The exponential amplitude is constrained

---

[3] Thanks to Dr. Arash Bahramian

to $0.4L_t \leqslant L_e \leqslant L_t$ based on Heinke et al. 2015. The linear shape is described by

$$F(t) = F_t \left(1 - \frac{t - t_t}{\tau_l} \right) \tag{7}$$

with $F(t)$ the count rate, F_t the count rate at the transition, t the time, t_t the time at the transition and τ_l the linear decay time. The final model thus looks like:

$$F(t) = \begin{cases} (6), & t \leqslant t_t. \\ (7), & t > t_t. \end{cases} \tag{8}$$

The model is fitted using Markov Chain Monte Carlo (*MCMC*) sampling. This is an improved version of the basic Monte Carlo sampling that produces a probability distribution from random start variables. The *MCMC* gives a probability distribution for each of the five parameters. The probability distribution lies between a chosen range and the meridian of the distribution is taken as the best fit value. Each parameter range is constraint by values matching with the outburst count rates.

Source selection
In order to fit this model to an outburst decay, the transition from a exponential to a linear decay must be clearly visible. In addition the number of data points at each side of the transition must be such that the difference between a totally exponential or linear decay is clear. For example some *Swift* light curves are having data points with intervals of one week which can't be used. However the *RXTE* light curves are have intervals of one day for which it is possible to distinct the exponential and linear part. The outbursts that meet these requirements are fitted with the decay model.

Accretion disk radius R_{circ}
With the fit parameters from this model several physical properties of the binary system can be derived. The first one is the radius of the accretion disk. This can be derived from

$$R_{disc} = 3.5 \times 10^7 \sqrt{\tau_e} \tag{9}$$

with R_{disc} the accretion disk radius and τ_e the exponential decay time (Heinke et al. 2015).

Orbital period P_{orb}
The second physical property that is determined is the orbital period P_{orb}. This orbital period is derived from the disc radius R_{disc} and the mass fraction q defined as the mass of the companion star divided by the mass of the compact object

$$P_{orb} = 3 \left(\frac{R_{disc}}{R_\odot} \right)^{3/2} \frac{1}{(1+q)^2} \frac{1}{[0.500 - 0.227 \log(q)]^6} h \tag{10}$$

with $R_\odot$ the mass of the Sun (Heinke et al. 2015).

Model validation
For sources with a known distance source d we are able to check if the model is corresponding to the theory with F_t. Therefore we converted count rates into flux with the Portable, Interactive Multi-Mission Simulator (*PIMMS*) tool (Mukai 1993)[4]. By replacing L_{acc} in equation 11 with the theoretical value from equations 1 or 2 and using the transition flux F_t from the fit we estimated the distance.

$$L_{acc} = 12\pi F d^2 \tag{11}$$

---

[4] https://heasarc.gsfc.nasa.gov/cgi-bin/Tools/w3pimms/w3pimms.pl

5 Results

5.1 Outburst detection

In total we found 41 outbursts in 21 sources listed in table 1. For each source we noted their confirmed compact object type, BH or a NS, in column 2. Sources with unknown compact object type are labeled with question mark. For each outburst the telescope used for observation and the time at the peak of the outburst is noted in column 2 and 3 respectively.

In total 5 outbursts were classified as unsuitable to determine the duration or decay time via fitting:

- Two sources, IGR J17597-2201 and XTE J1744-230, contain outbursts with variable count rates longer than one year, they are classified as quasi persistent (QP) outbursts. The high variability of QP outbursts makes them unsuitable to determine the duration or decay time.

- The light curve of IGR J17451-3022 also shows high variability in outburst so estimating the duration and decay time via fitting is not a realistic approximation.

- The *Swift* light curve of SAX J1828.5-1037 shows a clear outburst at MJD 55875. But this outburst contains only data points at the peak of the outburst which would result in big errors on the fit parameters.

- XTE J1719-356 shows one clear increased count rate at MJD 55376 in the *RXTE* light curve. The *Swift* light curve contains increased activity around the same time, shown in figure 4, which indicates that the increased activity in the *RXTE* light curve is real. Despite this increased activity, in the *RXTE* light curves there is now outburst shape visible besides this single data point. Additionally the *Swift* light curve does not show a clear outburst shape also due to few data points. This makes it too hard to conclude anything about the duration or decay time of this outburst.

lightcurves/lc_joined_XTEJ1719-356_ob.png

Fig. 4: The *RXTE* and *Swift* light curve of XTE J1719-356 show increased activity around MJD 55377. This indicates that there is a outburst.

5.2 Duration

In total 36 outbursts were successfully fitted to Gaussian function. The Gaussian fit of XTE J1728-295 is shown in figure 5.

gaussians/gauss_55388_XTEJ1728-295_RXTE.png

Fig. 5: Gaussian fit of a outburst from XTE J1728-295

Five outbursts (MJD 58584 XTE J1728-295, MJD 56010 IGR J1817-3656, MJD 55595 Swift J1357.2-0933, MJD 57868 Swift J1357.2-0933 and MJD 54644 XMMJ174457-2850.3) weren't fit to a Gaussian because they only contain the decay part. The duration extracted from the fits is shown in column $_5$ of table 1. The distribution of the duration from all outbursts can be seen in figure 6.
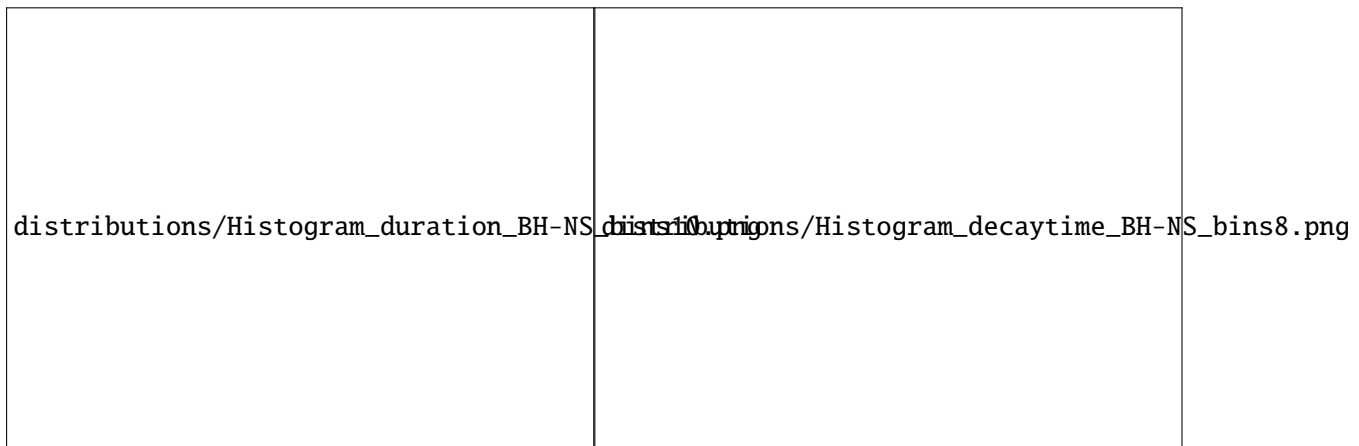
distributions/Histogram_duration_BH-NS_distributions/Histogram_decaytime_BH-NS_bins8.png

Fig. 6: Distribution of the outburst duration.   **Fig. 7:** Distribution of the outburst decay time.

5.3 Decay time

In total 40 outbursts were successfully fitted to a exponential function. The Exponential fit of XTE J1728-295 is shown in figure 8.

exponentials/exp_55388_XTEJ1728-295_RXTE.png

Fig. 8: Exponential fit of a outburst from XTE J1728-295

The outburst of IGR J17375-3022 at MJD 52466 has too few data points to resolve the outburst decay shape and produces a nonphysical decay time of 0.01. So this outburst decay time was excluded for analysis.

1 Source	2 BH/NS	3 Telescope	4 t_{peak} (MJD)	5 τ_{dur} r (days)	6 τ_{dec} (days)	7 Notes
XTE J1734-234	?	RXTE	51403	18.48	10.54	
IGR J17375-3022	?	RXTE	52466	5.940	0.01	
		RXTE	54750	7.380	2.41	
		RXTE	55043	7.440	1.89	
IGR J17597-2201	NS	RXTE	-	-	-	QP
		Swift	-	-	-	QP
SAX J1753.5-2349	NS	RXTE	51392	17.70	4.43	
		RXTE	54753	20.22	5.99	
		RXTE	55276	55.50	12.76	
WGA J1715.3-2635	?	RXTE	52501	113.72	26.86	
XTE J1118+480	BH	RXTE	51549	37.80	12.37	
	BH	RXTE	51693	321.51	76.31	
XTE J1637-498	?	RXTE	53215	17.70	2.73	
		RXTE	53818	29.90	3.28	
		RXTE	54707	30.20	5.67	
XTE J1719-291	NS	RXTE	54547	20.94	4.47	
XTE J1719-356	NS	RXTE	55376	-	-	U
		Swift	55379	-	-	U
XTE J1728-295	BH	RXTE	52927	261.45	22.21	
		RXTE	55440	135.62	59.77	
		Swift	58584	-	30.58	
XTE J1737-376	NS	RXTE	53053	15.33	3.05	
		RXTE	54714	21.09	7.09	
XTE J1744-230	?	RXTE	-	-	-	QP
IGR J1817-155	?	RXTE	54354	61.23	7.90	
IGR J1817-3656	BH	Swift	56010	-	11.26	
IGR J17451-3022	?	Swift	57056	-	-	HV
IGR J17494-3030	NS	Swift	56010	24.81	4.31	
SAX J1828.5-1037	?	Swift	55875	-	-	U
Swift J1357.2-0933	BH	Swift	55595	-	30.74	
		Swift	57868	-	35.86	
XMMJ174457-2850.3	NS	Swift	54644	-	2.53	
		Swift	55103	12.96	1.47	
		Swift	55408	10.09	2.24	
		Swift	56153	16.06	2.48	
		Swift	57659	13.89	2.77	
Swift J174553.7-290347	NS	Swift	53894	12.31	3.66	
Swift J174540.7-290015	?	Swift	57460	242.94	36.75	
Swift J174540.2-290037	?	Swift	57556	46.17	7.86	
		Swift		107.05	12.15	
Swift J174540.2-285921	?	Swift	55746	14.40	3.16	
		Swift	57578	16.61	2.93	
GRS 1741-2853	NS	Swift	54174	53.09	3.20	
		Swift	55112	40.76	5.02	
		Swift	55462	76.20	4.71	
		Swift	56517	33.19	2.21	
		Swift	57485	34.41	3.20	
		Swift	58045	24.39	7.77	

Tab. 1: All sources with their identified outbursts. For each source the type of compact object BH, NS or unkown is specified. For each outburst we noted from which telescope the observation data originates, the time at the peak of the outburst, the outburst duration, the outburst decay time and possible notifications. Notes dictionary; QP: Quasi persistant outburst, U: Unclear outburst shape due to few data points which make it unsuitable for fitting and HV: High Variability in outburst making it not suitable for fitting.

5.4 Decay model

1	2	3	4	5	6
Source	F_t	F_e	τ_e	τ_l	t_t
	$(c\ s^{-1})$	$(c\ s^{-1})$	(days)	(days)	(MJD)
SAX J1753.5-2349	32.434 ± 0.046	30.479 ± 0.054	5.999 ± 0.562	7.954 ± 0.572	55298.3 ± 1.1
XTE J1118+480	2.291^*	2.133 ± 0.01	3.382 ± 0.707	18.452 ± 1.346	51556.3 ± 0.8
XTE J1118+480	2.291 ± 0.01	2.275 ± 0.01	15.801 ± 6.357	30.735 ± 4.681	51727.0 ± 3.1
XTE J1737-376	20.845 ± 0.034	10.093 ± 0.080	6.124 ± 0.331	1.935 ± 0.530	54728.4 ± 0.5
XTE J1728-295	$4.571\ 10^{-11} \pm 0.012$	$2.009\ 10^{-11} \pm 0.033$	20.216 ± 0.685	92.049 ± 1.850	58629.3 ± 1.4
IGR J17177-3656	$1.652\ 10^{-1} \pm 0.041$	$6.855\ 10^{-2} \pm 0.045$	10.863 ± 0.250	15.877 ± 1.376	55662.1 ± 1.4
XMM J174457-2850.3	$3.273\ 10^{-2} \pm 0.115$	$1.706\ 10^{-2} \pm 0.155$	2.242 ± 0.238	3.975 ± 0.831	54651.3 ± 0.8

SAX J1753.5-2349

Equation 9 gives a disk radius of $2.520\ 10^{10}$ cm. This source is known as a NS binary so we assumed that $q = 0.1$. This disc radius together with the mass ratio gives a orbital period of 3.656 ± 0.342 h via equation 10.

decayfit/SAXJ1753.5-2349_pr.png
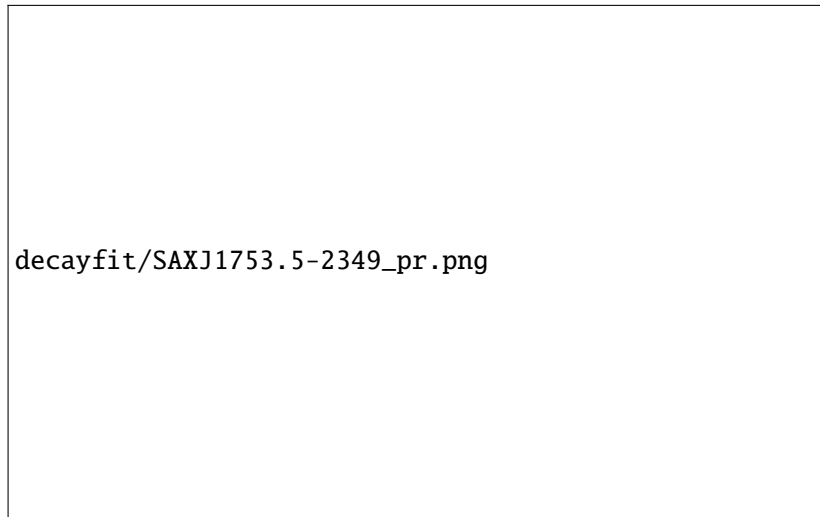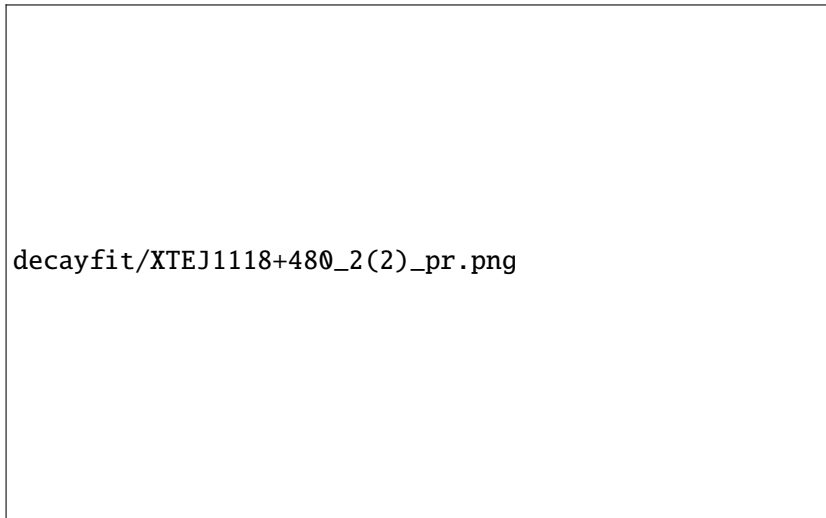
Fig. 9: Decay model fit of SAX J1753.5-2349
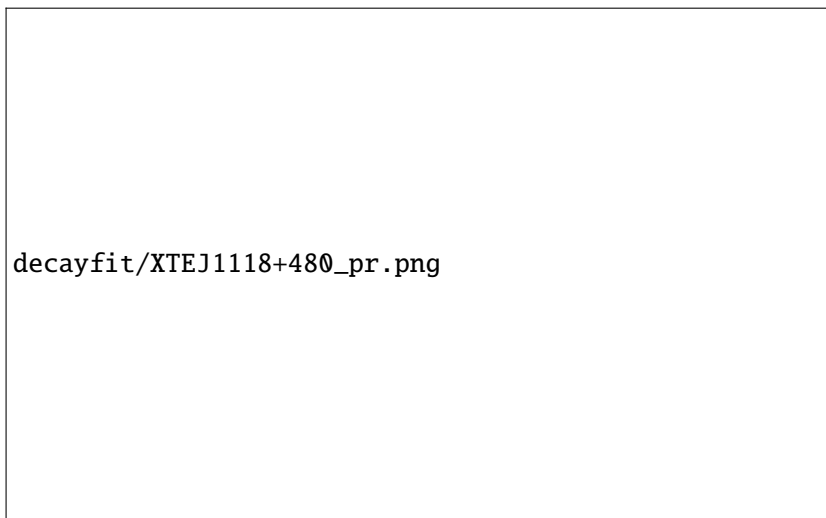
XTE J1118+480

There are two outbursts from XTE J1118+480 visible in its light curve. The fit of the outburst at MJD 51693 gives a disk radius of $4.089\ 10^{10}$ cm by equation 9. This disc radius together with a mass fraction 0.037 ± 0.007 give a orbital period of 3.4h$\pm$0.7 via equation 10. Analysis on the outburst at MJD 53215 can be found in the discussion. Based on the transition flux F_t this source should be at a distance of 3.074 ± 0.037 kpc with $N_h = 0.99\ 10^{22}$ based on Stoop et al. 2021.

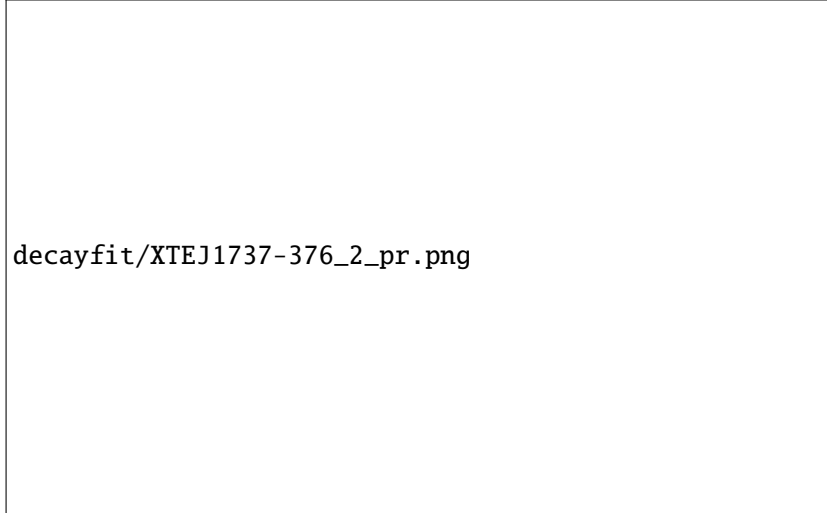**Fig. 10:** Decay model fit of XTE J1118+480

Fig. 11: Decay model fit of XTE J1118+480

XTE J1737-376

Equation 9 gives a disk radius of 2.546 10^{10} cm. This disc radius together with a mass ratio of $q = 0.04$ (Sanna et al. 2018) gives a orbital period of 2.05$\pm$0.10h via equation 10.
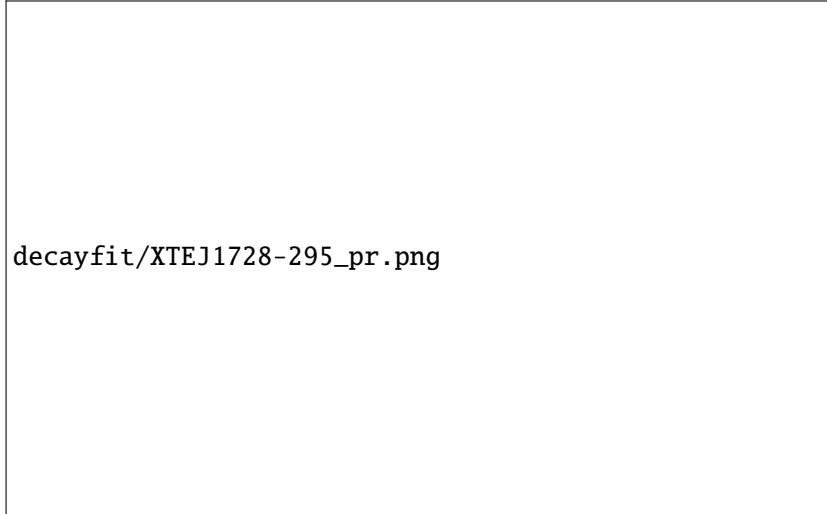
decayfit/XTEJ1737-376_2_pr.png

Fig. 12: Decay model fit of XTE J1737-376

XTE J1728-295

Assuming $q = 0.01$ gives a orbital period of 2.17 ± 0.05h via equation 10 as in Stoop et al. 2021.

decayfit/XTEJ1728-295_pr.png

Fig. 13: Decay model fit of XTE J1728-295

IGR J17177-3656

Equation 9 gives a disk radius of $3.390 \, 10^{10}$ cm. This disc radius together with a mass ratio of $q = 0.1$ gives a orbital period of 5.70 ± 0.13h via equation 10.
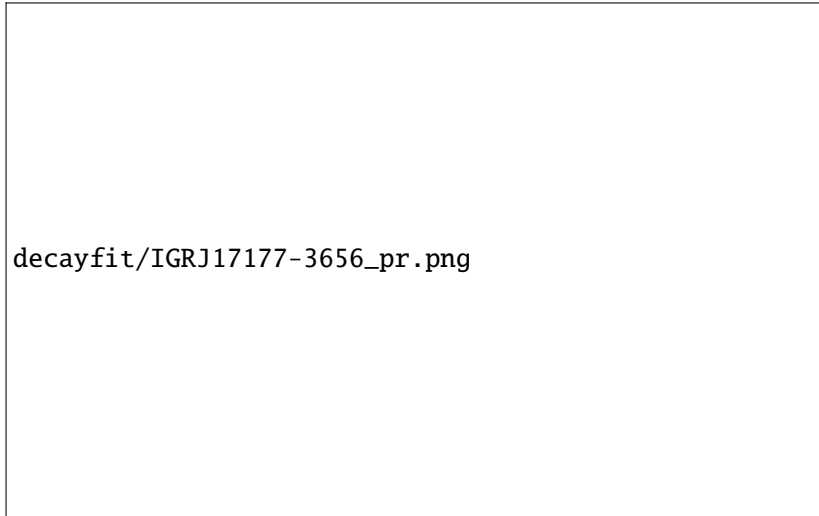
Fig. 14: Decay model fit of IGR J17177-3656

XMMJ174457-2850.3

Assuming $q = 0.1$ gives a orbital period of 1.81 ± 0.12h via equation 10 as in Heinke et al. 2015.
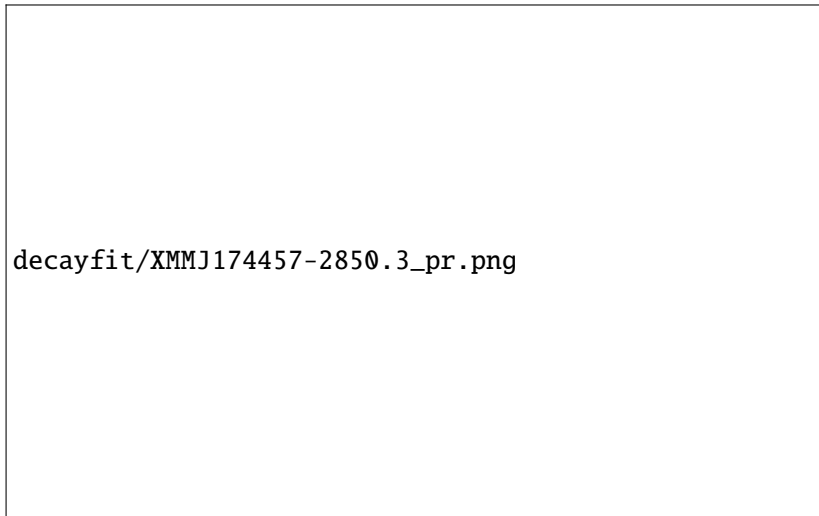
Fig. 15: Decay model fit of XMMJ174457-2850.3

6 Discussion

6.1 Typical duration and decay time

The duration and decay time distribution shows a similar trend to that of brighter sources (Yan and Yu 2015). This gives indications for a similar accretion process in both bright and very faint sources. Still it are indications since it is low number statistics. Secondly we noticed that BH's seems to have longer outbursts and decay times. Most BH's we observe are having a large accretion discs and

therefore longer outbursts and decay times which explains the difference between NSs and BHs in the distributions Wu et al. 2010.

It has to be mentioned that **?** used other methods to determine the duration and decay time. We have tested their method on WGAJ1715.3-2635 and found a duration more than 6 times larger than our selected outburst region. In their method they are selecting data points above a certain percentage from the peak rate. But because most light curves from VFXBs have low count rates and therefore higher noise levels this method turned out to be not useful.

6.2 Orbital periods

For all 6 sources we have found orbital periods of 1.81h to 5.70h which matches with the expectation from Wu et al. 2010. For XTE J1118+480 we obtained a distance of 3.074$\pm$0.037 kpc which is matching with observations ranging from 3 to 8 kpc (Gandhi et al. 2019). Also we checked the transition luminosity by fitting the first outburst to the decay model while fixing F_t to the value of the second outburst. This fit is shown in figure 11 and it seems a reasonable fit indicating the transition luminosity is the same in both outbursts. For XTE J1737-376 the orbital period was found to be 2.05$\pm$0.10h which matches witch $\sim$1.9h from Sanna et al. 2018. This gives indications that the disc instability model can be used for VFXBs that show a clear transition.

Most outbursts do not contain enough data points which makes the identification of a transition from exponential to linear decay difficult. Also in most light curves of VFXBs count rates are low and therefore hard to conclude if the model is working better than a complete linear or exponential for example. But for 7 outbursts the results look promising combined with the fact that observations match on 2 sources giving strong indications the decay model works. Therefore it is interesting to use and test the validity of this model further on future outbursts.

7 Conclusion

We have performed a first systematic study of outburst light curves from 21 VFXBs. Similar trends as in bright X-ray binaries in the distribution for the duration and decay time were found indicating a similar accretion process. BHs seem to have longer outbursts and decay times explained by the larger accretion disks of BHs. Using the disc instability model we have found orbital periods of 2 to 6 hours which as expected also indicating no different accretion process. For two sources the disc instability model predicts an orbital period and distance matching with observations. So far data quality is the most limiting factor to fit the disc instability model but more outburst showing enough data points to identify a transition are needed to test the instability model at a more convincingly way.

References

Astropy Collaboration and Thomas P. Robitaille. Astropy: A community Python package for astronomy. , 558:A33, October 2013. doi: 10.1051/0004-6361/201322068.

Luca Baiotti, Bruno Giacomazzo, and Luciano Rezzolla. Accurate evolutions of inspiralling neutron-star binaries: Prompt and delayed collapse to a black hole. *Phys. Rev. D*, 78:084033, Oct 2008. doi: 10.1103/PhysRevD.78.084033. URL https://link.aps.org/doi/10.1103/PhysRevD.78.084033.

Wan Chen, C. R. Shrader, and Mario Livio. The Properties of X-Ray and Optical Light Curves of X-Ray Novae. , 491(1):312–338, December 1997. doi: 10.1086/304921.

R. Cornelisse, F. Verbunt, J. J. M. in't Zand, E. Kuulkers, J. Heise, R. A. Remillard, M. Cocchi, L. Natalucci, A. Bazzano, and P. Ubertini. BeppoSAX Wide Field Cameras observations of six type I X-ray bursters. , 392:885–893, September 2002. doi: 10.1051/0004-6361:20020707.

J. M. Corral-Santana, J. Casares, T. Muñoz-Darias, F. E. Bauer, I. G. Martínez-Pais, and D. M. Russell. Blackcat: A catalogue of stellar-mass black holes in x-ray transients. *Astronomy Astrophysics*, 587: A61, Feb 2016. ISSN 1432-0746. doi: 10.1051/0004-6361/201527130. URL `http://dx.doi.org/10.1051/0004-6361/201527130`.

N. Degenaar and R. Wijnands. The behavior of subluminous X-ray transients near the Galactic center as observed using the X-ray telescope aboard Swift. , 495(2):547–559, February 2009. doi: 10.1051/0004-6361:200810654.

N. Degenaar, R. Wijnands, M. T. Reynolds, J. M. Miller, D. Altamirano, J. Kennea, N. Gehrels, D. Haggard, and G. Ponti. THE PECULIAR GALACTIC CENTER NEUTRON STAR x-RAY BINARY XMM j174457-2850.3. *The Astrophysical Journal*, 792(2):109, aug 2014. doi: 10.1088/0004-637x/792/2/109. URL `https://doi.org/10.1088/0004-637x/792/2/109`.

N. Degenaar, R. Wijnands, J. M. Miller, M. T. Reynolds, J. Kennea, and N. Gehrels. The Swift X-ray monitoring campaign of the center of the Milky Way. *Journal of High Energy Astrophysics*, 7: 137–147, September 2015. doi: 10.1016/j.jheap.2015.03.005.

P. A. Evans, A. P. Beardmore, K. L. Page, L. G. Tyler, J. P. Osborne, M. R. Goad, P. T. O'Brien, L. Vetere, J. Racusin, D. Morris, D. N. Burrows, M. Capalbi, M. Perri, N. Gehrels, and P. Romano. An online repository of Swift/XRT light curves of γ-ray bursts. , 469(1):379–385, July 2007. doi: 10.1051/0004-6361:20077530.

Juhan Frank, Andrew King, and Derek J. Raine. *Accretion Power in Astrophysics: Third Edition*. 2002.

Poshak Gandhi, Anjali Rao, Michael A. C. Johnson, John A. Paice, and Thomas J. Maccarone. Gaia Data Release 2 distances and peculiar velocities for Galactic black hole transients. , 485(2):2642–2655, May 2019. doi: 10.1093/mnras/stz438.

J.-M. Hameury and J.-P. Lasota. Outbursts in ultracompact x-ray binaries. *Astronomy Astrophysics*, 594:A87, Oct 2016. ISSN 1432-0746. doi: 10.1051/0004-6361/201628434. URL `http://dx.doi.org/10.1051/0004-6361/201628434`.

J.M. Hameury. A review of the disc instability model for dwarf novae, soft x-ray transients and related objects. *Advances in Space Research*, 66(5):1004–1024, 2020. ISSN 0273-1177. doi: https://doi.org/10.1016/j.asr.2019.10.022. URL `https://www.sciencedirect.com/science/article/pii/S0273117719307586`. Nova Eruptions, Cataclysmic Variables and Related Systems: Challenges in the 2020 Era.

C. O. Heinke, A. Bahramian, N. Degenaar, and R. Wijnands. The nature of very faint X-ray binaries: hints from light curves. *Monthly Notices of the Royal Astronomical Society*, 447(4):3034–3043, 01 2015. ISSN 0035-8711. doi: 10.1093/mnras/stu2652. URL `https://doi.org/10.1093/mnras/stu2652`.

Craig O. Heinke, Haldan N. Cohn, and Phyllis M. Lugger. THE DISCOVERY OF a VERY FAINT x-RAY TRANSIENT IN THE GLOBULAR CLUSTER m15. *The Astrophysical Journal*, 692

(1):584–593, feb 2009. doi: 10.1088/0004-637x/692/1/584. URL `https://doi.org/10.1088/0004-637x/692/1/584`.

in 't Zand, J. J. M., Jonker, P. G., and Markwardt, C. B. Six new candidate ultracompact x-ray binaries. *A&A*, 465(3):953–963, 2007. doi: 10.1051/0004-6361:20066678. URL `https://doi.org/10.1051/0004-6361:20066678`.

A. R. King and R. Wijnands. The faintest accretors. *Monthly Notices of the Royal Astronomical Society: Letters*, 366(1):L31–L34, 02 2006. ISSN 1745-3925. doi: 10.1111/j.1745-3933.2005.00126.x. URL `https://doi.org/10.1111/j.1745-3933.2005.00126.x`.

A.R. King and H. Ritter. The light curves of soft X-ray transients. *Monthly Notices of the Royal Astronomical Society*, 293(1):L42–L48, 01 1998. ISSN 0035-8711. doi: 10.1046/j.1365-8711.1998.01295.x. URL `https://doi.org/10.1046/j.1365-8711.1998.01295.x`.

Jean-Pierre Lasota. The disc instability model of dwarf novae and low-mass X-ray binary transients. , 45(7):449–508, June 2001. doi: 10.1016/S1387-6473(01)00112-9.

Q. Z. Liu, J. van Paradijs, and E. P. J. van den Heuvel. A catalogue of low-mass X-ray binaries in the Galaxy, LMC, and SMC (Fourth edition). , 469(2):807–810, July 2007. doi: 10.1051/0004-6361:20077303.

K. Mukai. PIMMS tool. *Legacy*, 3:21–31, October 1993.

M. P. Muno, J. R. Lu, F. K. Baganoff, W. N. Brandt, G. P. Garmire, A. M. Ghez, S. D. Hornstein, and M. R. Morris. A remarkable low-mass x-ray binary within 0.1 parsecs of the galactic center. *The Astrophysical Journal*, 633(1):228–239, nov 2005. doi: 10.1086/444586. URL `https://doi.org/10.1086/444586`.

Mason Ng, Paul S. Ray, Peter Bult, Deepto Chakrabarty, Gaurava K. Jaisawal, Christian Malacaria, Diego Altamirano, Zaven Arzoumanian, Keith C. Gendreau, Tolga Güver, Matthew Kerr, Tod E. Strohmayer, Zorawar Wadiasingh, and Michael T. Wolff. NICER Discovery of Millisecond X-Ray Pulsations and an Ultracompact Orbit in IGR J17494-3030. , 908(1):L15, February 2021. doi: 10.3847/2041-8213/abe1b4.

A. T. Okazaki and I. Negueruela. A natural explanation for periodic X-ray outbursts in Be/X-ray binaries. , 377:161–174, October 2001. doi: 10.1051/0004-6361:20011083.

Craig R. Powell, Carole A. Haswell, and Maurizio Falanga. Mass transfer during low-mass X-ray transient decays. , 374(2):466–476, January 2007. doi: 10.1111/j.1365-2966.2006.11144.x.

A. Sanna, E. Bozzo, A. Papitto, A. Riggio, C. Ferrigno, T. Di Salvo, R. Iaria, S. M. Mazzola, N. D'Amico, and L. Burderi. Xmm-newton detection of the 2.1 ms coherent pulsations from igr j17379–3747. *Astronomy Astrophysics*, 616:L17, Aug 2018. ISSN 1432-0746. doi: 10.1051/0004-6361/201833205. URL `http://dx.doi.org/10.1051/0004-6361/201833205`.

T. Shahbaz, P. A. Charles, and A. R. King. Soft X-ray transient light curves as standard candles: exponential versus linear decays. , 301(2):382–388, December 1998. doi: 10.1046/j.1365-8711.1998.01991.x.

Jean Swank and Craig Markwardt. Populations of Transient Galactic Bulge X-ray Sources. 251:94, January 2001.

B. E. Tetarenko, G. R. Sivakoff, C. O. Heinke, and J. C. Gladstone. Watchdog: A comprehensive all-sky database of galactic black hole x-ray binaries. *The Astrophysical Journal Supplement Series*, 222(2):15, Feb 2016. ISSN 1538-4365. doi: 10.3847/0067-0049/222/2/15. URL `http://dx.doi.org/10.3847/0067-0049/222/2/15`.

M. A. P. Torres, P. J. Callanan, M. R. Garcia, P. Zhao, S. Laycock, and A. K. H. Kong. MMT observations of the black hole candidate XTE j1118480 near and in quiescence. *The Astrophysical Journal*, 612(2):1026–1033, sep 2004. doi: 10.1086/422740. URL `https://doi.org/10.1086/422740`.

Derek Tournear, E. Raffauf, Elliott Bloom, W. Focke, B. Giebels, Gary Godfrey, Pablo Saz Parkinson, Kaice Reilly, K. Wood, P. Ray, M. Wolff, Reba Bandyopadhyay, Michael Lovellette, and Jeffrey Scargle. X-ray bursts in neutron star and black hole binaries from unconventional stellar aspect experiment and rossi x-ray timing explorer data: Detections and upper limits. *The Astrophysical Journal*, 595:1058, 12 2008. doi: 10.1086/377431.

R. Wijnands, J. J. M. in 't Zand, M. Rupen, T. Maccarone, J. Homan, R. Cornelisse, R. Fender, J. Grindlay, M. van der Klis, E. Kuulkers, and et al. Thexmm-newton/chandramonitoring campaign of the galactic center region. *Astronomy Astrophysics*, 449(3):1117–1127, Mar 2006. ISSN 1432-0746. doi: 10.1051/0004-6361:20054129. URL `http://dx.doi.org/10.1051/0004-6361:20054129`.

Y. X. Wu, W. Yu, T. P. Li, T. J. Maccarone, and X. D. Li. Orbital Period and Outburst Luminosity of Transient Low Mass X-ray Binaries. , 718(2):620–631, August 2010. doi: 10.1088/0004-637X/718/2/620.

Zhen Yan and Wenfei Yu. X-Ray Outbursts of Low-mass X-Ray Binary Transients Observed in the RXTE Era. , 805(2):87, June 2015. doi: 10.1088/0004-637X/805/2/87.

8 Apendix

8.1 Light curves

lightcurves/lc_XTEJ1734-234_RXTE.png

lightcurves/lc_IGRJ17375-3022_RXTE.png

lightcurves/lc_joined_IGRJ17597-2201.png

lightcurves/lc_SAXJ1753.5-2349_RXTE.png

lightcurves/lc_WGAJ1715.3-2635_RXTE.png

lightcurves/lc_XTEJ1734-234_RXTE.png

lightcurves/lc_XTEJ1118+480_RXTE.png

lightcurves/lc_XTEJ1637-498_RXTE.png

lightcurves/lc_XTEJ1719-291_RXTE.png

lightcurves/lc_joined_XTEJ1719-356.png

lightcurves/lc_joined_XTEJ1728-295.png

lightcurves/lc_XTEJ1737-376_RXTE.png

lightcurves/lc_XTEJ1744-230_RXTE.png

lightcurves/lc_XTEJ1817-155_RXTE.png

lightcurves/lc_IGRJ17177-3656_Swift.png

lightcurves/lc_IGRJ17451-3022_Swift.png

lightcurves/lc_IGRJ17494-3030_Swift.png

lightcurves/lc_SAXJ1828.5-1037_Swift.png

lightcurves/lc_SwiftJ1357.2-0933_Swift.png

lightcurves/lc_XMMJ174457-2850.3_SwiftGC.png

lightcurves/lc_SwiftJ174553.7-290347_SwiftGC.png

lightcurves/lc_SwiftJ174540.7-290015_SwiftGC.png

lightcurves/lc_SwiftJ174540.2-290037_SwiftGC.png

lightcurves/lc_SwiftJ174535.5-285921_SwiftGC.png

```
lightcurves/lc_GRS1741-2853_SwiftGC.png
```

8.2 Gaussian fits

```
gaussians/gauss_51392_XTEJ1734-234_RXTE.png
```
```
gaussians/gauss_52415_IGRJ17375-3022_RXTE.png
```

```
gaussians/gauss_54733_IGRJ17375-3022_RXTE.png
```
```
gaussians/gauss_55035_IGRJ17375-3022_RXTE.png
```

```
gaussians/gauss_51382_SAXJ1753.5-2349_RXTE.png
```
```
gaussians/gauss_54744_SAXJ1753.5-2349_RXTE.png
```

gaussians/gauss_55265_SAXJ1753.5-2349_RXTE.png

gaussians/gauss_52427_WGAJ1715.3-2635_RXTE.png

gaussians/gauss_51537_XTEJ1118+480_RXTE.png

gaussians/gauss_51603_XTEJ1118+480_RXTE.png

gaussians/gauss_54525_XTEJ1719-291_RXTE.png

gaussians/gauss_52826_XTEJ1728-295_RXTE.png

gaussians/gauss_55388_XTEJ1728-295_RXTE.png
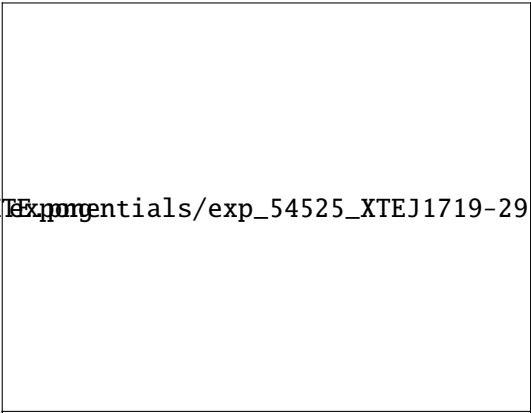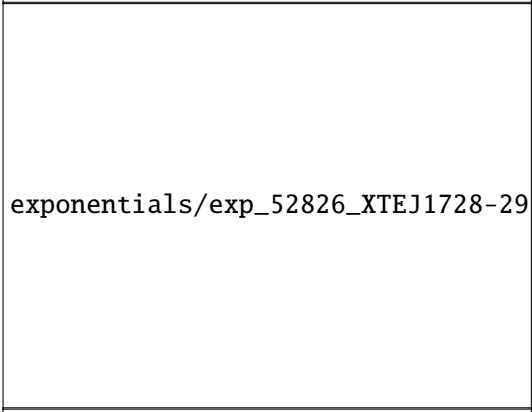
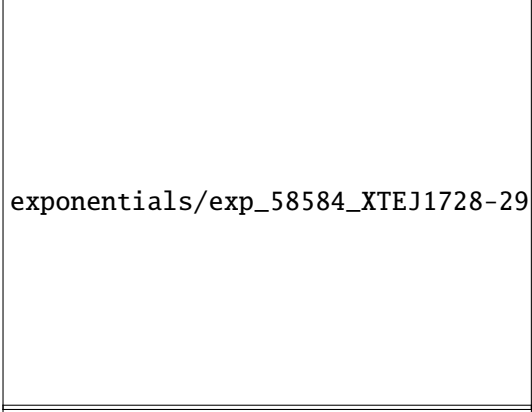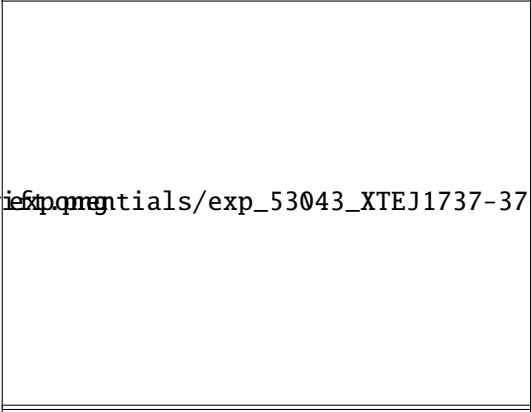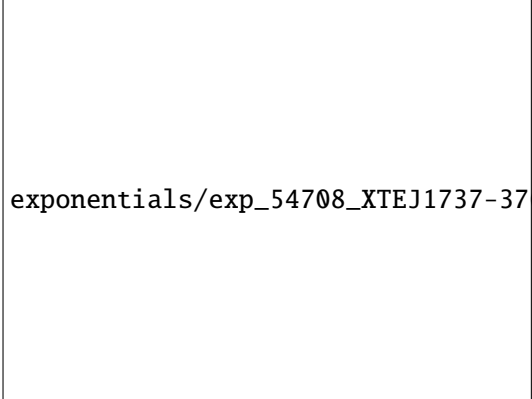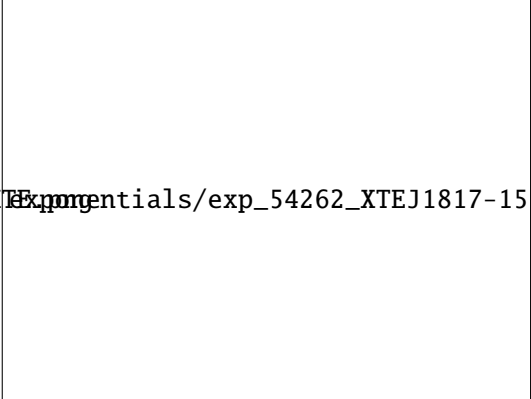gaussians/gauss_53043_XTEJ1737-376_RXTE.png
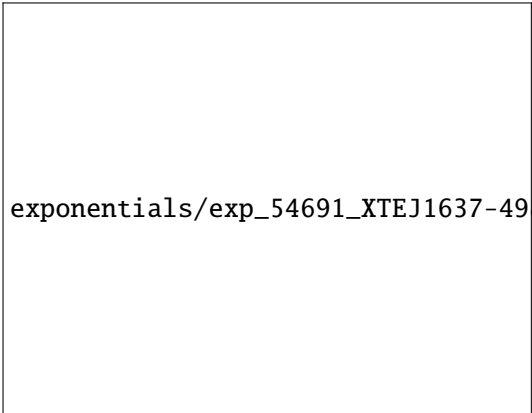
gaussians/gauss_54708_XTEJ1737-376_RXTE.png gaussians/gauss_54262_XTEJ1817-155_RXTE.png

gaussians/gauss_56007_IGRJ17494-3030_SwiftGC.png gaussians/gauss_55091_XMMJ174457-2850.3_SwiftGC.p

gaussians/gauss_55383_XMMJ174457-2850.3_SwiftGC.png gaussians/gauss_56099_XMMJ174457-2850.3_SwiftGC.p

gaussians/gauss_56135_XMMJ174457-2850.3_SwiftGC.png gaussians/gauss_57652_XMMJ174457-2850.3_SwiftGC.p

gaussians/gauss_53200_XTEJ1637-498_RXTE.png

gaussians/gauss_53783_XTEJ1637-498_RXTE.png

gaussians/gauss_54691_XTEJ1637-498_RXTE.png

8.3 Exponential fits

exponentials/exp_51392_XTEJ1734-234_RXTE.png

exponentials/exp_52415_IGRJ17375-3022_RXTE.png

exponentials/exp_54733_IGRJ17375-3022_RXTE.png

exponentials/exp_55035_IGRJ17375-3022_RXTE.png
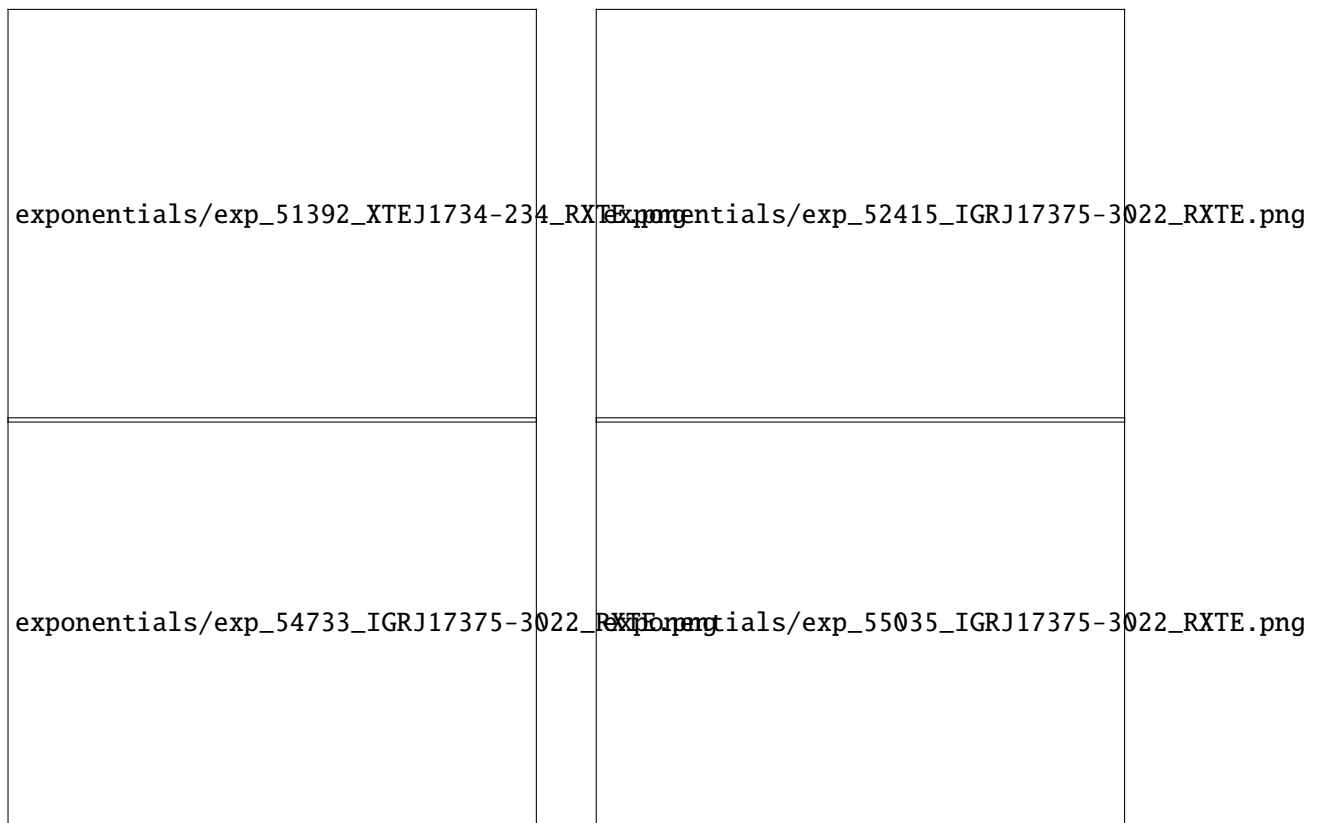
exponentials/exp_51382_SAXJ1753.5-2349_RXTE.png

exponentials/exp_54744_SAXJ1753.5-2349_RXTE.png

exponentials/exp_55265_SAXJ1753.5-2349_RXTE.png

exponentials/exp_52427_WGAJ1715.3-2635_RXTE.png

exponentials/exp_51537_XTEJ1118+480_RXTE.png

exponentials/exp_51603_XTEJ1118+480_RXTE.png

exponentials/exp_53200_XTEJ1637-498_RXTE.png

exponentials/exp_53783_XTEJ1637-498_RXTE.png

exponentials/exp_54691_XTEJ1637-498_RXTE.png exponentials/exp_54525_XTEJ1719-291_RXTE.png

exponentials/exp_52826_XTEJ1728-295_RXTE.png exponentials/exp_55388_XTEJ1728-295_RXTE.png

exponentials/exp_58584_XTEJ1728-295_Swift.png exponentials/exp_53043_XTEJ1737-376_RXTE.png

exponentials/exp_54708_XTEJ1737-376_RXTE.png exponentials/exp_54262_XTEJ1817-155_RXTE.png

exponentials/exp_55637_IGRJ17177-3656_Swift.png exponentials/exp_56906_IGRJ17451-3022_Swift.png

exponentials/exp_56007_IGRJ17494-3030_Swift.png exponentials/exp_55593_SwiftJ1357.2-0933_Swift.pn

exponentials/exp_57865_SwiftJ1357.2-0933_Swift.png exponentials/exp_54644_XMMJ174457-2850.3_SwiftGC.

exponentials/exp_55091_XMMJ174457-2850.3_SwiftGC.png exponentials/exp_55383_XMMJ174457-2850.3_SwiftGC.

exponentials/exp_56135_XMMJ174457-2850.exponentGCalpnxgexp_57652_XMMJ174457-2850.3_SwiftGC.

exponentials/exp_53890_SwiftJ174553.7-290347_Swiafts_GCexpng57310_SwiftJ174540.7-290015_Swif

exponentials/exp_57425_SwiftJ174540.2-290037_Swiafts_GCexpng57521_SwiftJ174540.2-290037_Swif

exponentials/exp_57521_SwiftJ174540.2-290037_Swiafts_GCexpng55667_SwiftJ174535.5-285921_Swif

exponentials/exp_57562_SwiftJ174535.5-285921_SwiftGC.png exponentials/exp_54186_GRS1741-2853_SwiftGC.png

exponentials/exp_55116_GRS1741-2853_SwiftGC.png exponentials/exp_55383_GRS1741-2853_SwiftGC.png

exponentials/exp_56528_GRS1741-2853_SwiftGC.png exponentials/exp_57491_GRS1741-2853_SwiftGC.png

exponentials/exp_58035_GRS1741-2853_SwiftGC.png